Influence of Cell Structure Parameters on the Mechanical Properties of Microcellular Polypropylene Materials

Wei Gong,[1,2,3] Jiacheng Gao,[1] Ming Jiang,[3] Li He,[3] Jie Yu,[3] Jianhua Zhu[3]

[1]*College of Materials Science and Engineering, Chongqing University, Chongqing 400030, China*
[2]*Department of Material and Building Engineering, Guizhou Normal University, Guiyang 550014, China*
[3]*National Engineering Research Center for Compounding and Modification Polymeric Materials, Guiyang 550014, China*

Received 13 May 2010; accepted 29 November 2010
DOI 10.1002/app.33874
Published online 6 July 2011 in Wiley Online Library (wileyonlinelibrary.com).

ABSTRACT: Microcellular polypropylene (PP) was prepared through chemical microcellular injection under different processing parameters. The effects of cell structure parameters on the mechanical properties of PP materials were analyzed by the microsphere model. The results show that the mechanical properties of microcellular PP with a smaller cell size and more uniform size distribution were enhanced. The relationship between the mechanical properties and cell structure parameters correlated well with the theoretical model. © 2011 Wiley Periodicals, Inc. J Appl Polym Sci 122: 2907–2914, 2011

Key words: computer modeling; composites; mechanical properties

INTRODUCTION

Microcellular polymer materials have attracted much attention because of their scientific interest and potential applications as packaging, construction, and insulation materials.[1,2] However, the large and nonuniform cells of the foams lead to obviously decreased mechanical properties.[3–6] Jacobs et al.[7] reported the effects of some parameters, including blowing agents and fillers, on the mechanical properties of plastics. Rachtanapun and coworkers[8,9] reported the effect of the cell structures of foamed polypropylene (PP)/polyethylene (PE) blends on the material properties, which indicated that the small and uniform cells resulted in improvements of the comprehensive properties. Zhang et al.[10] simulated the compression process of elastic open-cell foams by the Voronoi random model and found that the geometrical properties of the cells had significant influences on the mechanical behavior of the foams. Shulmeister and coworkers[11,12] found that the large-strain mechanical behavior of foams is dependent on the minimum effective cross section of the foam using the Voronoi technique and finite element analysis. Lu and Zhang[13] reported the numerical simulation of the tensile deformation process of low-density, open-cell elastic foams, which indicated the effect of the relative density of the foams on cell shape irregularity and the mechanical behaviors. These works focused on the relationship between cell structure and mechanical behavior; however, there are few reports of the relationship between cell size distribution and mechanical properties. Herein, we report a sphere model based on the virtual bearing area of cells in different sections to exhibit the influence of cell size and size distribution of foamed PP material on the mechanical properties at the same foaming ratio.

Correspondence to: J. Gao (gongwei1974@126.com).

Contract grant sponsor: Major State Basic Research Development Program of China; contract grant number: 2007CB616912.

Contract grant sponsor: National Natural Science Foundation of Guizhou Province; contract grant number: 2009J2020.

EXPERIMENTAL

Materials

PP T30S, a commercial product from Sinopec, was selected for this study. A foaming masterbatch and assistant masterbatch were prepared with the procedure described in our previous report[14] in a twin-screw extruder.

Preparation of the blowing agent masterbatch

The blowing agent masterbatch was prepared by the blending of azodicarbonamide and low-density PE in a twin-screw extruder. An approximate azodicarbonamide/low-density PE ratio of 10 : 90 (w/w)

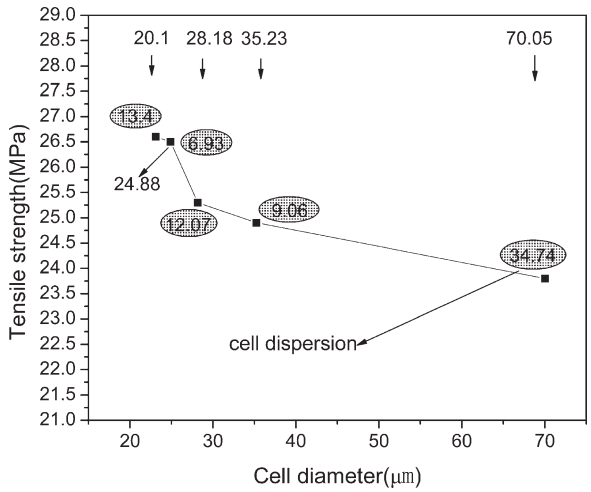

Figure 1 Effect of the cell size and distribution on the tensile strength of microcellular PP. The numbers in circles are the dispersions of the cell sizes.

was used. The masterbatch to be used was dried at 80°C for 12 h before melt processing.

Preparation of the additive masterbatch

The additive masterbatch was prepared by the mixing of zinc oxide (ZnO) and zinc stearate ($C_{36}H_{70}O_4Zn$) into the PE matrix in a twin-screw extruder. An approximate $ZnO/C_{36}H_{70}O_4Zn$ ratio of 75 : 25 (w/w) was used. The masterbatch to be used was dried at 80°C for 12 h before melt processing.

Preparation of the microcellular PP materials

Foamed standard tensile test bars (200 ×10 ×4.4 mm^3) were molded through a two-step molding process under various process conditions in an injection-molding machine. In this study, the blowing agent masterbatch and additive masterbatch were used at 15 and 5 wt % levels, respectively. The densities of the samples were determined by a Mettler Toledo balance. The density of the final foamed products was in the range of 0.808–0.813 g/cm^3, and the density of corresponding unfoamed samples was about 0.919 cm^3. After foaming, the density decreased by 12%.

Characterization

Determination of the cell size and size distribution

Scanning electron microscopy (SEM) was used to determine foam morphology. The samples were dipped in liquid nitrogen and then fractured to expose their cellular morphology, and the fracture surfaces were contrasted with gold before the characterization of foam structure. The SEM images of foamed samples were analyzed with Image-Pro Plus software (Media Cybernetic) to quantitatively assess cell size. The area and number of cells in the SEM images could be calculated by Image-Pro Plus software to obtain the average size of the cells. At least 100 cells in the SEM micrographs for each sample were used to evaluate the mean cell size and size distribution. A dispersion coefficient (S_d) is used to denote the distribution of cells in foamed material and can be calculated according to the equation of standard deviation, as follows:

$$S_d = \left\{ \sum_{i=1}^{n} (R_i - R)^2 / n \right\}^{1/2} \quad (1)$$

where n is the number of counted cells, R_i is the single cell diameter, and R is the average diameter of cells.

Mechanical measurement

Tensile strengths were determined according to Chinese standard GB/T1040.1-2006 with a tensile test machine (Instron 8510). Tests were performed at 24°C with a constant crosshead speed of 50 mm/min. Impact tests were conducted according to Chinese

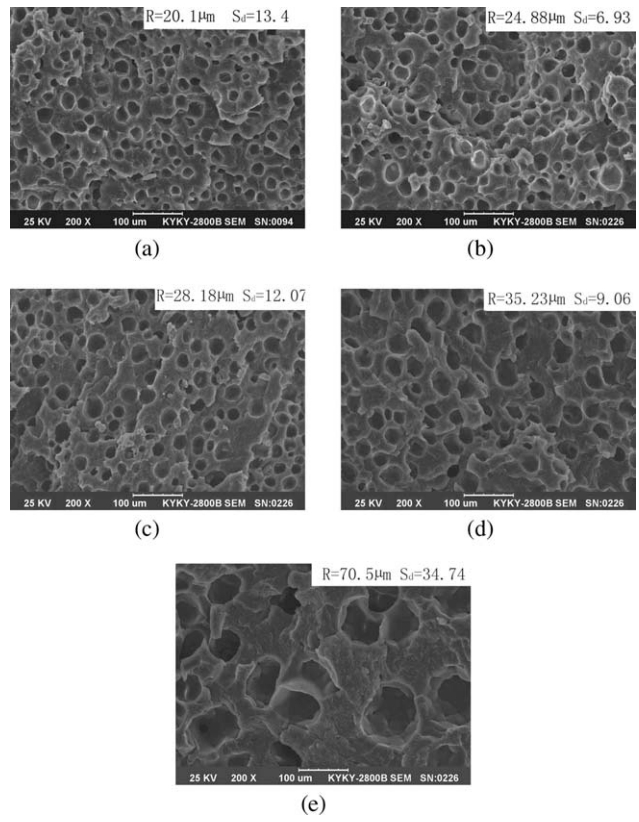

Figure 2 SEM images of the microcellular PP with different cell sizes and distributions.

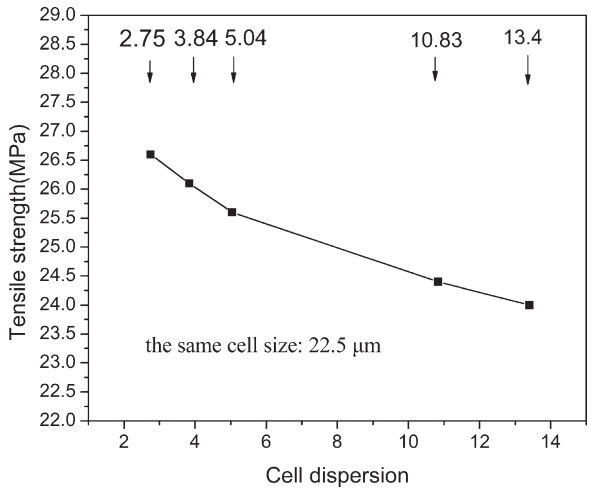

Figure 3 Effect of the cell distribution on the tensile strength of the microcellular PP with the same cell size.

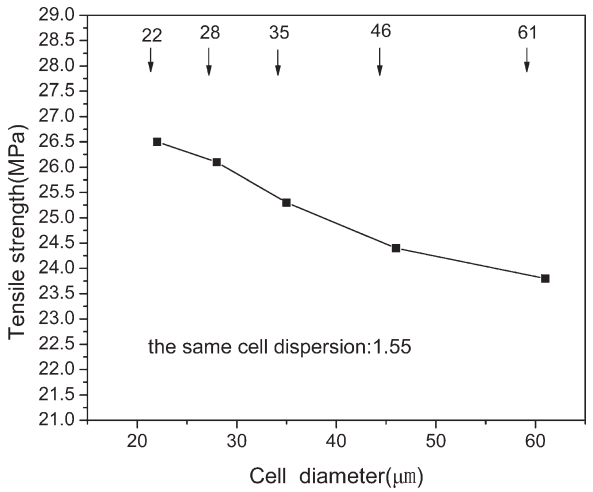

Figure 5 Effect of the cell size on the tensile strength of the microcellular PP with the same cell size S_d.

standard GB/T1843-2008 at 24°C on different cell size foam samples with a drop-weight impact test machine.

RESULTS AND DISCUSSION

Dependence of the mechanical properties on the cell size and distribution

Figure 1 illustrates the effect of the cell size and distribution on the mechanical properties, and the corresponding microstructures are shown in Figure 2. The tensile strength decreased with increasing cell size, whereas the difference of S_d's led to the nonlinear drop. This implied that the tensile strength was affected by both the cell size and distribution.

In Figure 3, the tensile strength is plotted versus cell S_d at the same average cell size, and the corresponding microstructures are shown in Figure 4. Figure 3 shows the linear drop in tensile strength

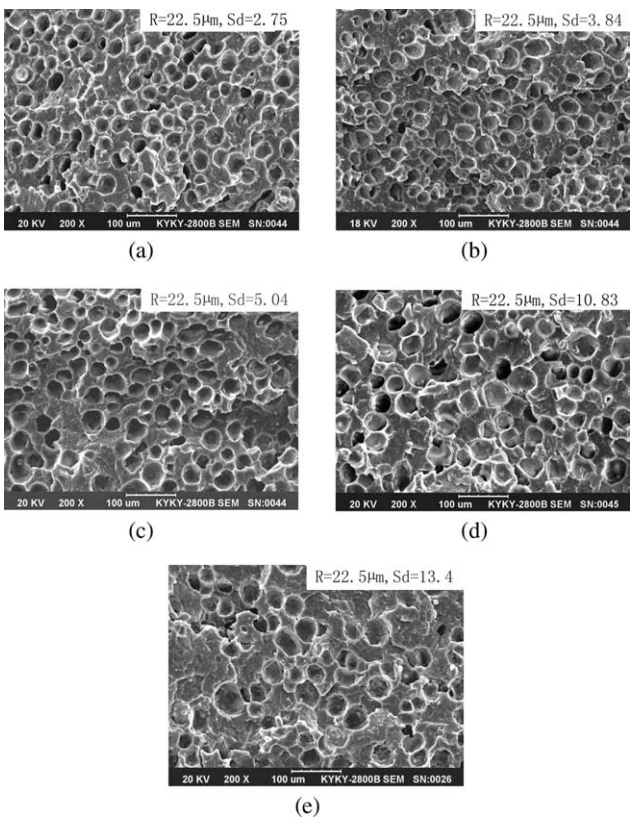

Figure 4 SEM images of the microcellular PP with different cell size S_d's.

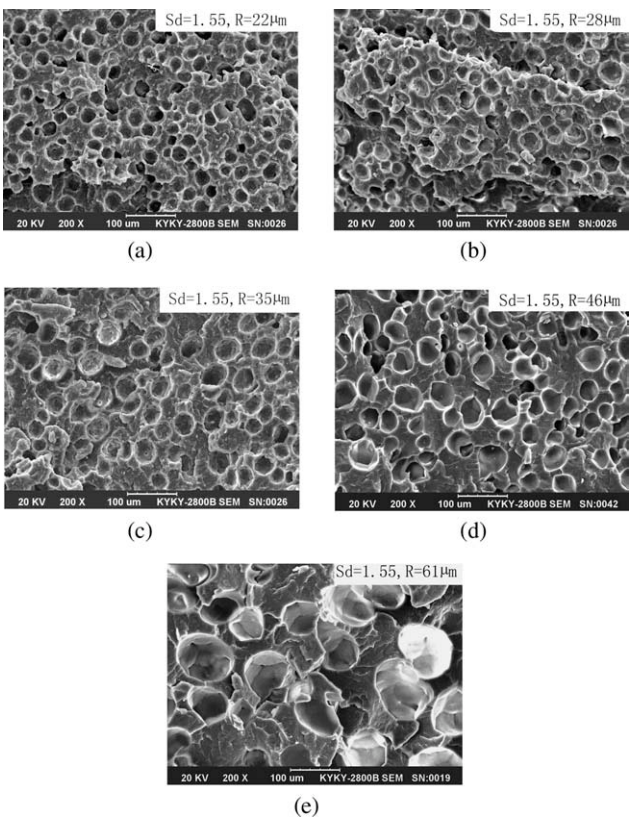

Figure 6 SEM images of the microcellular PP with different cell sizes.

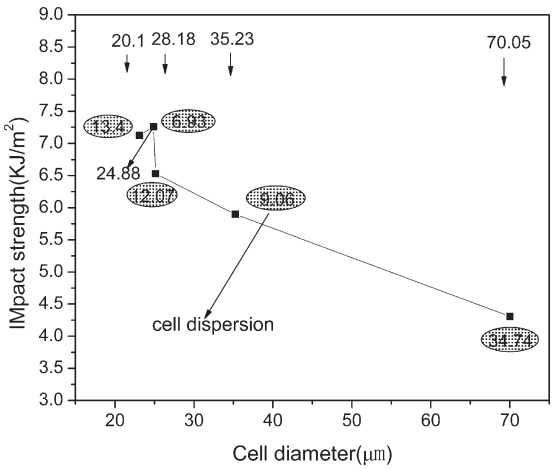

Figure 7 Effect of the cell size on the impact strength of the microcellular PP.

with S_d, which indicates the strong dependence of tensile strength on S_d.

Figure 5 shows the dependence of tensile strength on cell size at the same cell S_d, and the corresponding microstructures are shown in Figure 6. The tensile strength decreased with increasing cell size. Compared to cell distribution, cell size showed a stronger effect on the tensile strength; this indicated that fine cells facilitated the improvement of the tensile strength of microcellular PP.

Impact strength is the most important mechanical property index for characterizing polymers; it is used to measure the energy absorption of deformation and fracture when subjected to impact loading.[15–17] The effects of cell size and distribution on the impact strength of microcellular PP are shown in Figure 7. The trend observed was similar to that of tensile strength, which implied the dual effects of cell size and distribution on the impact strength.

As shown in Figure 8(a,b), respectively, the impact strength dropped with increasing average cell size or distribution.

Microsphere model

Model for microspheres with the same S_d and different Rs

Cells are modeled as spheres. The basic unit is assumed to be an ideal cube with the side length of $50t$, where t is designed as a proportional constant to represent the size of the cells. Several assumptions were made in this work for simplicity:[18–22] (1) all of the cells were spheres with a fixed diameter, (2) the cells were isotropic under stress, and (3) the cell walls were elastoplastic bodies.

As shown in Figure 9(a), the microspheres formed a body-centered cubic structure, and R was equal to $12t$. On the basis of the calculating formula of atoms in the body-centered cubic structure, the number of spheres in a basic unit (L) can be expressed as

$$L = 8 \times \frac{1}{8} + 1 = 2 \tag{2}$$

and

$$V_{\text{sphere}} = 2 \times \frac{4}{3}\pi R^3 = 2 \times \frac{4}{3}\pi(12t)^3 \approx 15,000t^3 \tag{3}$$

$$V_{\text{cube}} = a^3 = (50t)^3 = 125,000t^3 \tag{4}$$

where R is the radius of the microspheres and t is the proportional constant.

It is known by eqs. (3) and (4) that the volume of the spheres was 12% of that of basic cube. This

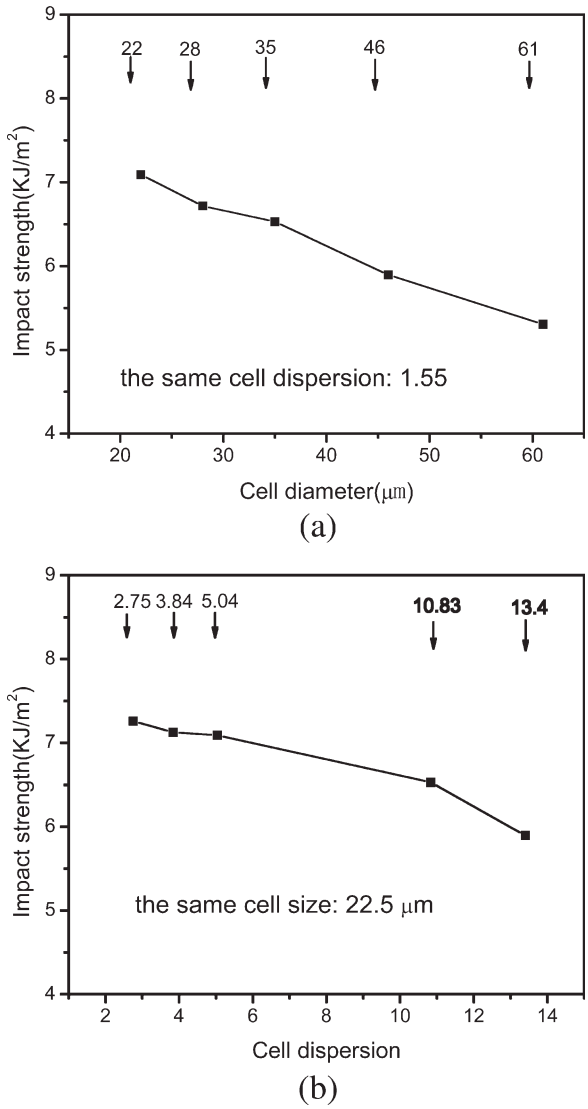

Figure 8 Effect of the cell dispersion on the impact strength of microcellular PP, where (a) R = 22.5 μm, different cell dispersion, and (b) S_d = 1.55, different cell size.

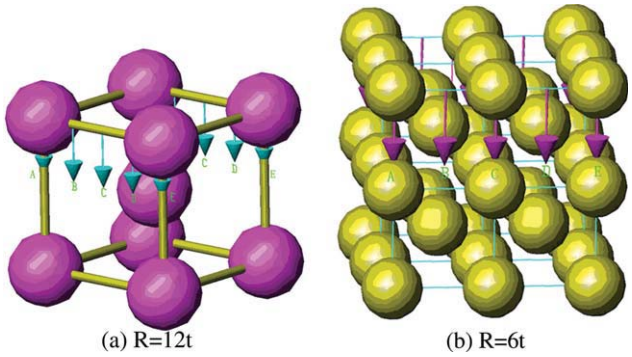

Figure 9 Model for microspheres with the same S_d and different *R*s. [Color figure can be viewed in the online issue, which is available at wileyonlinelibrary.com.]

volume was consistent with the 12% reduction in the density of the foamed PP.

In the case of Figure 9(b), $R = 6t$, the basic cube was divided into eight small body-centered cubic structures by the spheres. Each small cube contained two spheres, and thus, each basic cube was composed of 16 spheres. In this case

$$V_{\text{sphere}} = 16 \times \frac{4}{3}\pi R^3 = 16 \times \frac{4}{3}\pi(6t)^3 \approx 15,000t^3 \quad (5)$$

It could be easily calculated by eqs. (4) and (5) that the volume of spheres was still 12% of that of basic cube.

To validate the tensile and impact test results, five cross sections in the direction givens in Figure 9, A–A, B–B, C–C, D–D, and E–E, were obtained, and then, the cross sections shown in Figure 10 were intercepted, respectively, in the previous five cross sections at $3t$ intervals from the centerline. According to aforementioned method, five cross sections, including A–a–a, A–b–b, A–c–c, A–d–d, and a centered cross section vertical to A–A cross section, were obtained. Likewise, 1 vertical to B–B, 10 vertical to C–C, 1 vertical to D–D, and 5 vertical to E–E in Figure 9(a) were obtained, and in addition, 3 vertical to A–A, 1 vertical to B–B, 6 vertical to C–C, 1 vertical to D–D, and 3 vertical to E–E in Figure 9(b) were obtained. The section schematics of the microspheres shown in Figure 9(a,b) are presented in Figure 10(a,b), respectively.

The cross-sectional area of the sphere in each cross section was calculated, and the corresponding area curve is given in Figure 11. Herein, t was assigned a value of 1 to simplify the calculation. The virtual areas of the spheres in different cross sections could be calculated through the integration of the curves in Figure 11 and are presented in Table I.

For the larger spheres, the distribution of the virtual area in different directions is more nonuniform than that of the smaller spheres, which leads to stress concentration and, subsequently, initiates crack or even fracture. The relationship between the cell size and mechanical properties could be elucidated by the previous analysis.

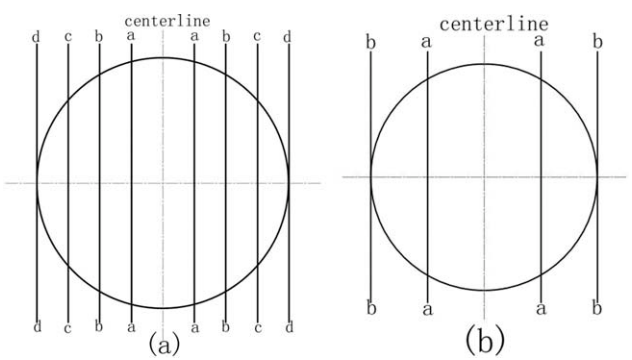

Figure 10 Section schematics of the microspheres.

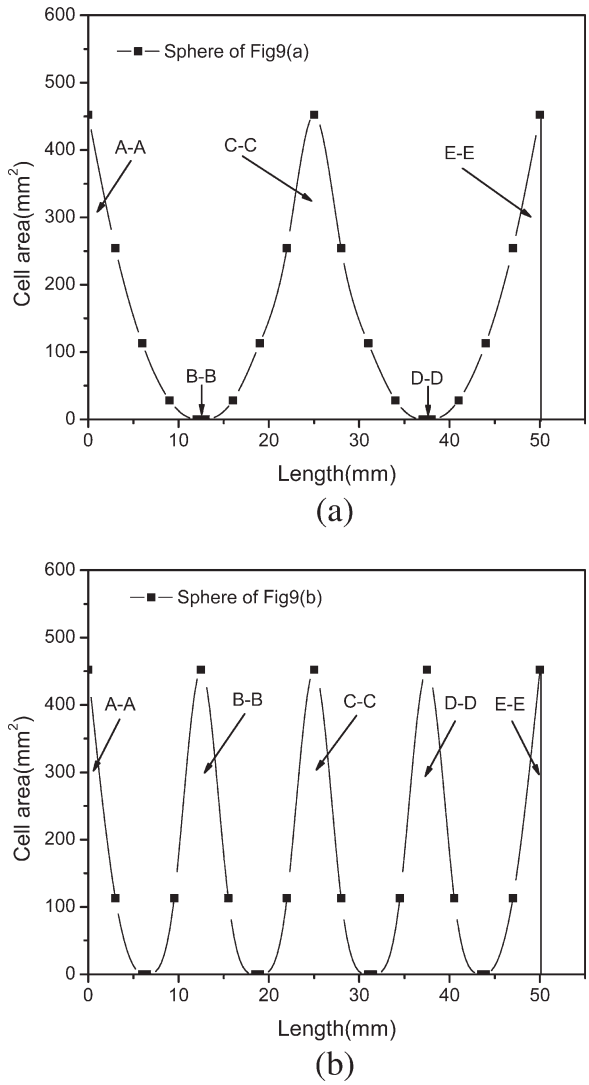

Figure 11 Area curve of the sphere in each cross section.

TABLE I
Virtual Area of Spheres with the Same S_d and Different Rs for Different Cross Sections

	Virtual area of the microspheres				
R	A–A	B–B	C–C	D–D	E–E
12t	1865.16t^2	0	3730.32t^2	0	1865.16t^2
6t	1017.36t^2	2034.72t^2	2034.72t^2	2034.72t^2	1017.36t^2

Model for microspheres with the same R and different S_d's

The three groups of microspheres shown in Figure 12 had the same average diameter. The condition of the model is consistent with that in Figure 9. The volume and cross-sectional area of the microspheres could be calculated according to eqs. (2)–(4), and the formula for the area of a circle is $S = \pi R^2$.

As shown in Figure 12(a), the microspheres formed a body-centered cubic structure, and R could be calculated on the basis of the number of microspheres in the cube at 12% of void fraction; namely, R_1 and R_2 were equal to 10t and 13.72t, respectively. When the previous values are substituted into Eq. (1), S_d is equal to 18.59t. The number of microspheres in the cubes is as follows:

$$L_1 = 8 \times \frac{1}{8} = 1$$

$$L_2 = 1$$

$$L = L_1 + L_2 = 2 \tag{6}$$

$$V_{\text{sphere}} = \sum_{i=1}^{2} \frac{4}{3}\pi R_i^3 = \frac{4}{3}\pi[(10t)^3 + (13.72t)^3] \approx 15,000t^3 \tag{7}$$

For the spheres in Figure 12(b), R_1, R_2, and S_d were equal to15t, 5.92t, and 45.4, respectively:

$$L = L_1 + L_2 = 2$$

$$V_{\text{sphere}} = \sum_{i=1}^{2} \frac{4}{3}\pi R_i^3 = \frac{4}{3}\pi[(15t)^3 + (5.92t)^3] \approx 15,000t^3 \tag{8}$$

For the spheres in Figure 12(c), R_1, R_2, and S_d were equal to 2t, 15.289t, and 93.97, respectively:

$$L = L_1 + L_2 = 2$$

$$V_{\text{sphere}} = \sum_{i=1}^{2} \frac{4}{3}\pi R_i^3 = \frac{4}{3}\pi[(2t)^3 + (15.289)^3] \approx 15,000t^3 \tag{9}$$

It was known from eqs. (3), (7), (8), and 9 that the volume of the spheres was 12% of that of the basic cube. This volume was consistent with the 12% reduction in the density of the foamed PP.

To analyze the dependence of the mechanical properties on the cell size distribution, five cross sections in the directions given in Figure 12(a), A–A, B–B, C–C, D–D, and E–E, were obtained and are given in Figure 13. Similar cross sections obtained from Figure 12(b,c) are shown in Figures 14 and 15, respectively.

The virtual cross-sectional areas of the spheres for different cross sections are given in Table II, where we can see that there was no sphere or cell on the cross sections B–B and D–D. The virtual cross-sectional areas of spheres first increased with S_d up to a maximum and then decreased for A–A and E–E, whereas for C–C, it was just the opposite. The largest value of the virtual cross-sectional area of spheres occurred on C–C when S_d was equal to 93.97 and where it was more prone to crack initiation because of the reduced bearing area. Therefore, we concluded that increased S_d resulted in more deteriorated mechanical properties.

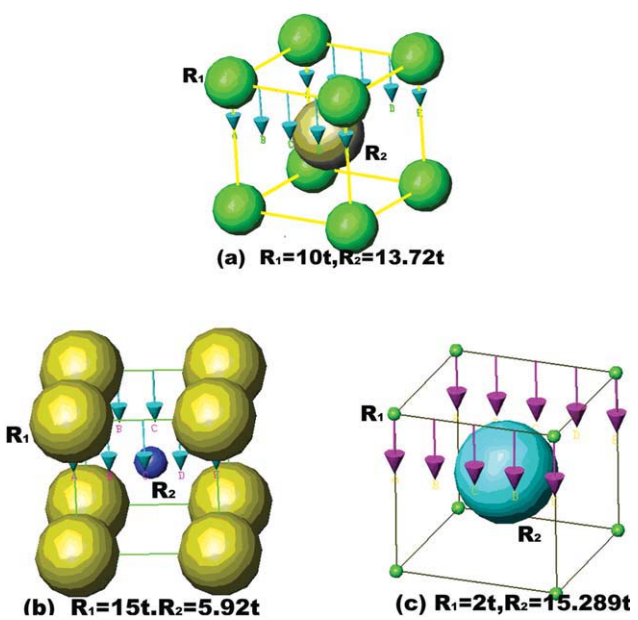

Figure 12 Model for microspheres with the same R and different S_d's. [Color figure can be viewed in the online issue, which is available at wileyonlinelibrary.com.]

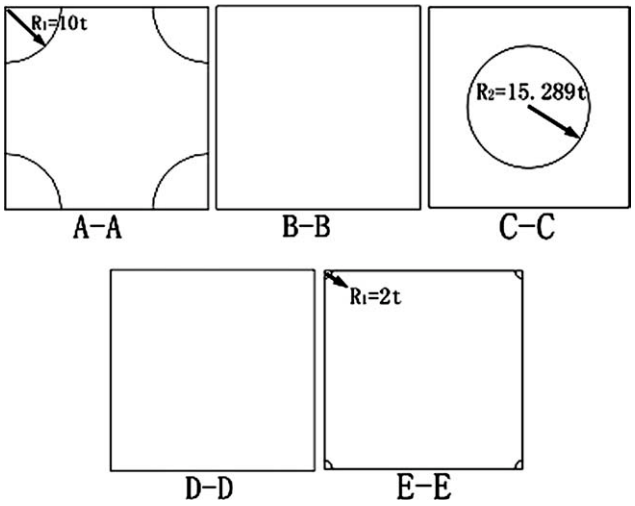

Figure 13 Section schematics in different directions for the model in Figure 12(a).

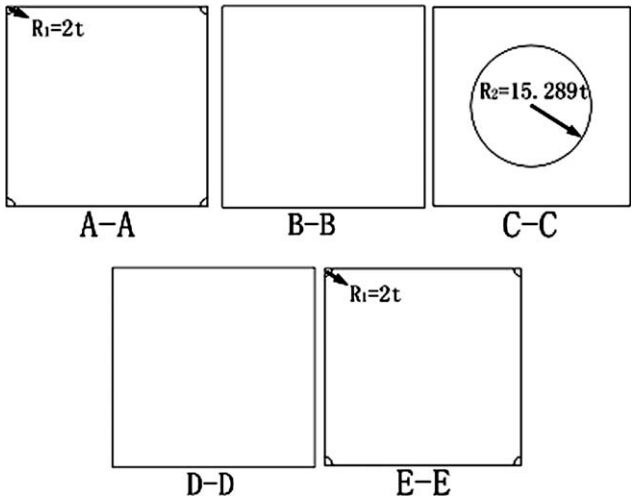

Figure 15 Section schematics in different directions for the model in Figure 12(c).

For the theoretical model, when the total cross-sectional area is invariant, the virtual cross-sectional areas of spheres with small size or narrow size dispersion at different cross sections are relatively small, or the remainder of the total cross-sectional area are relatively large. Correspondingly, for the foams, the reduced cell size or narrow size dispersion resulted in the increased virtual bearing area of foams for the case of constant void fraction and, sequentially, more favorable mechanical properties.

TABLE II
Virtual Area of Spheres with the Same *R* and Different S_d's for Different Cross Sections

	Virtual area of the microspheres				
S_d	A–A	B–B	C–C	D–D	E–E
18.59	$314t^2$	0	$314t^2$	0	$314t^2$
45.40	$705t^2$	0	$110.5t^2$	0	$705t^2$
93.97	$12.56t^2$	0	$733.99t^2$	0	$12.56t^2$

CONCLUSIONS

Microcellular PP with 12% of void fraction was prepared through chemical microcellular injection. A microsphere model was built on the basis of a fixed void fraction to predict the dependence of the mechanical properties on the cell size and distribution. The tensile and impact strengths of the foams with the same average cell size increased with diminishing cell size S_d, whereas those of the foams with the same cell size S_d increased with decreasing average cell size. For the theoretical model, when the total cross-sectional area is invariant, the virtual cross-sectional areas of spheres with small size or narrow size dispersion at different cross sections are relatively small, or the remainder of the total cross-sectional area is relatively large. The relationship between the mechanical properties and cell structure parameters correlated well with the theoretical model.

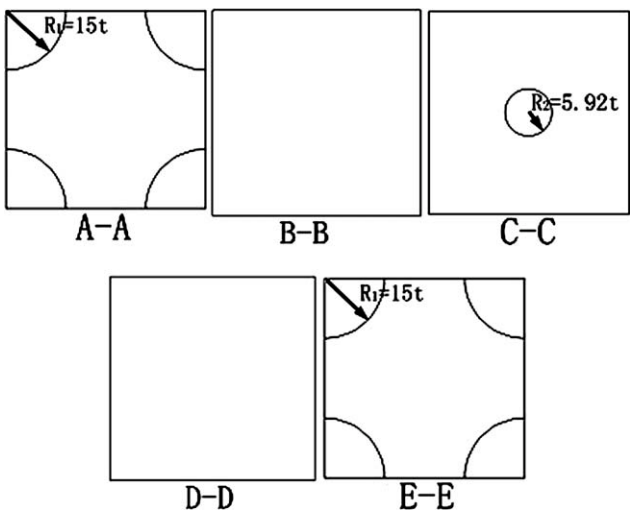

Figure 14 Section schematics in different directions for the model in Figure 12(b).

References

1. Kumar, V. Cell Polym 1993, 12, 207.
2. Throne, J. L. Thermoplastic Foams; Sherwood: Hinckley, OH, 1996.
3. Tejeda, E. H.; Sahagún, C. Z.; González-Núñez, R.; Rodrigue, D. J Cell Plast 2005, 41, 417.
4. Dubois, R.; Karande, S.; Wright, D. P.; Martinez, F. J Cell Plast 2002, 38, 149.
5. Cao, X.; Lee, J. L.; Widya, T.; Macosko, C. Polymer 2005, 46, 775.
6. Doroudiani, S.; Kortschot, M. T. J Appl Polym Sci 2003, 90, 1421.

7. Jacobs, M. A.; Kemmere, M. F.; Keurentjes, J. T. F. Polymer 2004, 45, 7539.
8. Rachtanapunp, P.; Matuana, L. M.; Selke, S. E. M. Soc Plast Eng Annu Tech Conf 2003, 61, 1762.
9. Rachtanapunp, P.; Selke, S. E. M.; Matuana, L. M. Polym Eng Sci 2004, 44, 1551.
10. Zhang, J.; Lu, Z. Chin J Aeronaut 2007, 20, 215.
11. Van der Burg, M. W. D.; Shulmeister, V.; Van der Geissen, E.; Marissen, R. J Cell Plast 1997, 33, 31.
12. Shulmeister, V.; Van der Burg, M. W. D.; Van der Giessen, E.; Marissen, R. Mech Mater 1998, 30, 125.
13. Lu, Z.; Zhang, J. J Mech Strength 2009, 31, 432.
14. Gong, W.; Gao, J. C.; Jiang, M.; Yu, J.; He, L. Int Polym Process 2010, 25, 270.
15. Kim, T. H.; Lim, S. T.; Lee, C. H.; Choi, H. J.; Jhon, M. S. J Appl Polym Sci 2003, 87, 2106.
16. Yuan, M.; Turng, L.; Gong, S.; Caulfield, D.; Hunt, C.; Spindler, R. Polym Eng Sci 2004, 44, 673.
17. Rodríguez-Pérez, M. A.; Velasco, J. I.; Arencón, D.; Almanza, O.; De Saja, J. A. J Appl Polym Sci 2000, 75, 156.
18. Xu, J.; Kishbaugh, L. J Cell Plast 2003, 39, 29.
19. Bureau, M. N.; Champagne, M. F.; Gendron, R. J Cell Plast 2005, 41, 73.
20. Sovboda, P.; Zeng, C.; Wang, H.; Lee, L. J.; Tomasko, D. L. J Appl Polym Sci 2002, 85, 1562.
21. Doroudiani, S.; Kortschot, M. T. J Appl Polym Sci 2003, 90, 1421.
22. Doroudiani, S.; Kortschot, M. T. J Appl Polym Sci 2003, 90, 1427.